Utilizations of Reaction Exothermic heat to Compensate The Cost of The Permanent CO2 Sequestration through the Geological Mineral CO2 Carbonation

Mingwei Ouyang
Guangzhou Institute of Energy Conversion
Yan Cao (caoyan@ms.giec.ac.cn)
Guangzhou Institute of Energy Conversion

Article

Keywords: geological mineral CO2 carbonation, mineral carbonation, CO2 sequestration rate, reaction exotherm, sequestration cost

Posted Date: June 22nd, 2022

DOI: https://doi.org/10.21203/rs.3.rs-1757895/v1

Utilizations of Reaction Exothermic heat to Compensate The Cost of The Permanent CO_2 Sequestration through the Geological Mineral CO_2 Carbonation

Ouyang Mingwei[1,2], Yan Cao*[1,2,3]

[1]Guangdong Provincial Key Laboratory of New and Renewable Energy Research and Development, Guangzhou Institute of Energy Conversion, Chinese Academy of Sciences, Guangzhou 510640, China.

[2]University of Science and Technology of China, No.96, JinZhai Road Baohe District, Hefei, Anhui, 230026, P.R.China.

[3]College of Chemistry and Chemical Engineering, Anhui University, Hefei 230601, China

*Correspondence: caoyan@ms.giec.ac.cn (Y. Cao)

Abstract: Many climate change events related to the carbon emissions push the worldwide action on the CO_2 sequestration to achieve the carbon neutrality. Among of them, the must-do list includes the CO_2 geological storage which has potentials on the leakage of the sequestrated CO_2 back to atmosphere. The new "geological mineral CO_2 carbonation" provides an alternative routine to rapidly sequester CO_2 by means of chemical reactions, and thus to permanently store CO_2 as the stable carbonates. The exothermic nature of the mineral carbonation reaction can release recoverable heat which can potentially compensate the energy consumption during the CO_2 sequestration. This study mainly addresses a two-dimensional model on the geological mineral CO_2 carbonation (herein the geological formation of peridotite), by which effects of temperature conditions on the reaction rate and their quantity of the sequestrated CO_2 and exothermic heat energy are discussed. Results reveals a typical case of the average temperature elevation of peridotite by over 60 ^oC (reaching 248^oC) after 2 years, in case of the initial temperature of the geological peridotite formation at 185^oC and that of the fluid inflow CO_2 at 37^oC. In this typical case, the average CO_2 sequestration rate in peridotite can achieve 123.71 kg/(year·m^3), meaning that the permanent sequestration of CO_2 generated from a 600 MW coal-fired power plant within its 20-year operation only demands a geological peridotite formation of 1 km^2 in its area and 160 m in its thickness. By changing both the fluid inflow temperature and the initial peridotite temperature to be 110~150^oC, the average CO_2 sequestration rate can be increased by 29~45% compared to that in the typical case, and leads to a temperature rise of 81~125^oC after 2 years, achieving a high-temperature geothermal condition which the temperature is greater than 150^oC. This heat production from the geological mineral CO_2 carbonation can profitably compensate the energy consumption in the carbon capture and storage (CCS) projects via the geological mineral CO_2 carbonation, leading a shift of an expense in \$25.041/t CO_2 in China (the current general case) to an earning in \$24.096/t CO_2 in a best case at the price of the global carbon emission allowance converge.

Keywords: geological mineral CO_2 carbonation, mineral carbonation, CO_2 sequestration rate, reaction exotherm, sequestration cost

1. Introduction

International authority confirms that human activities in emitting greenhouse gases are warming the atmosphere, oceans and land [1], triggering global climate change and leading massive human and economic losses [2,3], and thus urgently demanding CO_2 to be controlled and prevented from emitting into atmosphere [4]. The Chinese annual carbon emissions from the fossil energy consumption is 10 billion tons and announces its obligation to reduce carbon emissions with a setting goal of the achieved carbon neutrality by 2060 [5]. This vast carbon emissions contrasts to the estimated Chinese forest carbon sinks in only 190 to 340 million tons of CO_2 per year [6], implying clearly much less carbon sink than its emissions and highly demanding on the CO_2 capture and storage (CCS) to achieve the goal of the carbon neutrality [7]. Technically, CCS refers to the capture and injection and storage of carbon in deep geological reservoirs such as deep saline formation (DSF) or the profitably enhanced oil recovery (EOR), as shown in Supplementary Information Fig. S1 (SI Fig. 1). In geological reservoirs, the captured and injected CO_2 is physically sealed in the porous rock below the impermeable cap, preventing it from emit into atmosphere. This regular storage conditions may change due to those such as earthquakes, leading the sequestered CO_2 again return to atmosphere [8]. CCS not only involves the technical factor, also other major factors such as the long-term safety, public acceptance as well as economics [9].

Seifritz proposed the in-situ mineral carbonation to minimize the risk of leakage of sequestered CO_2 to achieve permanent CO_2 sequestration [10]. This accelerated CO_2 reaction with selected minerals can be achieved in geological sites of alkali-silicate to form alkali-carbonates and the silicate rocks is topped by impermeable caprocks and non-reactive overlying rocks, as shown in Supplementary Information Fig. S2 (SI Fig. 2). They are extremely stable and environmentally friendly in the geological environment [11,12], even under naturally acidic and high temperature geothermal conditions [13]. Natural silicate minerals for the potential sequestration of CO_2 can be olivine, serpentine, basaltic glass, and calcareous feldspar [14,15]. Among of them, basal and ultramafic rocks (e.g., peridotite with olivine as the main component) remains the most-likely potential CO_2 injection sequestration formations considering their vast reservoirs, wide distribution, highly-rich in alkali elements, fast reaction rates and thus relatively lower engineering costs [16].

Peridotite is selected in this study because of its fastest carbonation rate under geological sequestration conditions [17]. The main component to react CO_2 in peridotite is Mg_2SiO_4, its carbonation reactions can be simplified to equation (1). Most importantly, the mineral carbonation reaction is found to be exothermic in 760 kJ/kg of peridotite (in the ambient condition), which is about 3 times of the exothermic heat of serpentinization. Fig. 1 shows a mapping on the distribution of peridotites and ophiolites in China [18] (the ophiolites are actually composed of mantle peridotites).

$$Mg_2SiO_4+2CO_2 \rightarrow 2MgCO_3+SiO_2 \quad (1)$$

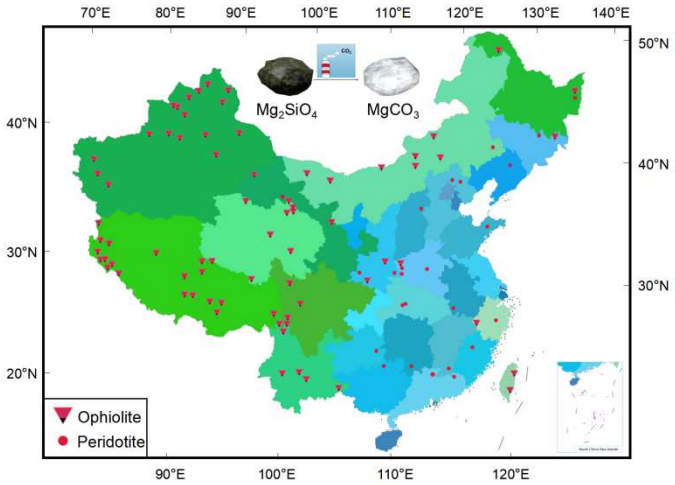

Fig. 1. The mapping of the distribution of ophiolites and peridotites in China

The economics factor is major reason hindering the CO_2 geological storage projects worldwide. In China, the majority CO_2 sequestration projects are difficult to generate revenue except for those likely profitable enhanced oil recovery (EOR) projects via the CO_2 sequestration. This is why the generation of exothermic heat during the CO_2 sequestration is interesting if heat can be fully utilized to compensate for the energy consumption. It's expected that the release heat will accumulate in the stratum for a long time because of the low thermal conductivity of the rocks. A study roughly estimates the heat energy utilization via a one-dimensional model while maintaining the peridotite temperature at 185°C [19] and the further likely power generations [20], addressing none of crucial mass and heat transfers on the CO_2 reaction rate and exothermic heat under realistic conditions. The missing information is crucially involved into the economics estimates on the geological mineral CO_2 carbonation, a chance to generate "artificial geothermal heat" during the carbon capture and storage (CCS).

This study established a two-dimensional transient model on the geological mineral CO_2 carbonation using peridotite, involving the CO_2 percolation, heat and mass transfers and CO_2 mineral carbonation reactions. The simulation revealed effects of critical temperature conditions on rates of CO_2 sequestration reactions and their exothermic nature, achieving the best technical routines toward the realization of the reaction energy utilize under more realistic conditions. Results inspired the likelihood on a profitable economics via the geological mineral CO_2 carbonation upon the validation on the permanent stability of the stored CO_2 and its safety. Significantly, the heat generation during the geological mineral CO_2 carbonation realize a high-temperature geothermal condition (> 150°C), which not only compensates the cost of the CCS and even make profits.

2. Modeling method

In this study, the multi-physics field coupled simulation software COMSOL Multiphysics was used to numerically simulate the carbonation process of peridotite based on the finite element method. COMSOL has been widely used to solve problems in the geosciences [21]. A peridotite formation at a depth of 1000 m in Uyghur Autonomous Region, China, was studied as an example. The vertical section of the stratum in this realistic simulation model is shown in Supplementary Information Fig. S3 (SI Fig. 3). The peridotite is topped by impermeable caprocks and non-reactive overlying rocks.

A two-dimensional process simulation was considered in views of the feasibility and effectiveness of the numerical calculation. The size of the peridotite area is 1000 m by 1000 m in its section, and an injection well in a diameter of 0.1 m is setup at the center of the lower boundary of the peridotite area. The peridotite is surrounded by an outer layer of non-reactive rocks (hereafter referred as outer rocks), and the distance between the inner and outer boundaries is 500 m. The geometric model is shown in Fig. 2. The simulation area is grided into grid cells using grid refinement techniques in COMSOL. The selection of the grid numbers is tested in views of the simulation accuracy and efficiency, leading the acceptable mesh division of 4392 domain units, and the average grid cell quality is 0.7412. Fig. 3 shows a selected mesh division drawing.

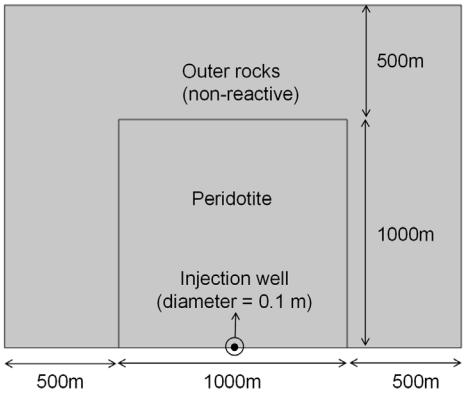

Fig. 2. Geometric model

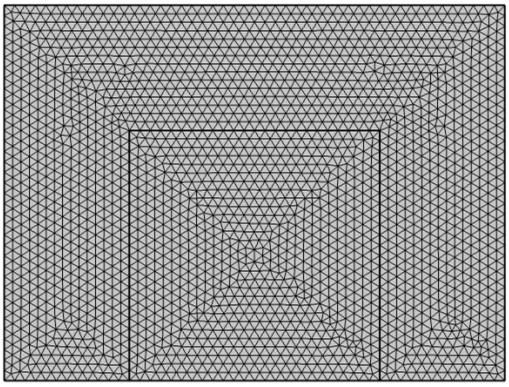

Fig. 3. Diagram of the mesh division

Supplementary Information Table. S1 (SI Table. 1) shows the typical parameters of peridotite used in the modelling [22]. The Mg_2SiO_4 content of peridotite was conservatively taken to be 40 %. The outer rocks is not reacted with CO_2, but same as peridotite in other involving physical properties. The temperature of the outer rocks at 1000 m is setting 37°C (the average annual temperature of the ground in Xinjiang plus 30°C/km geothermal gradient). The physical and chemical properties of CO_2 are from the National Institute of Standards (NIST) Chemistry WebBook. Pressure at the bottom of the injection well is 10 MPa, and the pressure at the starting point of CO_2 pipeline transportation is setting 15 MPa. The amount of CO_2 transportation and injection is regulated via the CO_2 sequestration rate or reaction rate. Table. 1 shows the temperature setting conditions in this study, hereafter referring the fluid inflow temperature and initial peridotite temperature to be Tin and T0, respectively (187°C is set as the temperature upper limit to facilitate parametric scanning calculations, which can be regarded as the same as 185°C).

Table. 1. The different temperature conditions used in this study

Case	The fluid inflow temperature (Tin, °C)	The initial peridotite temperature (T0, °C)
Typical	37 (temperature of outer rocks in the 1000 m deep)	185 (best carbonation reaction temperature of peridotite)
Varying Tin	37	37~187
Varying T0	37~187	185
Varying Tin&T0	37~187	37~187

The simulation assumptions are as followed,

(1) The porosity and permeability of peridotite do not change as the reaction proceeds, as shown in previous studies [23,24].

(2) The physical properties of CO_2 only vary with temperature, because its properties are more sensitive to temperature rather than pressure in the study range.

(3) The rock temperature and CO_2 temperature are equal at each point of simulation area, and heat transfer is dominated by both the conduction and convection and the thermal radiation can be ignorable under current lower temperatures.

(4) The peridotite has been preheated to its best carbonation reaction temperature of 185°C, while the demanding energy can be selectively from ventilated flue gas of nearby power plants , the high-temperature geothermal [25], the post-combustion oilfield associated gas, and the solar collector.

Based on the above assumptions, the mathematical equations involve the mass conservation control equation, the seepage field control equation and the temperature field control equation.

(1) The percolation field is controlled by the COMSOL's built-in "Darcy's Law" application modules, represented by following equations,

$$\frac{\partial（\epsilon_p \rho）}{\partial t}+\nabla\cdot(\rho u)=Q_m \quad (2)$$

$$u=-\frac{\kappa}{\mu}\nabla p \quad (3)$$

where ρ is the fluid density (unit: kg/m^3), ε is the rock porosity, μ is the viscosity (unit: Pa·s), κ is the permeability of porous media (unit: m^2), and p is the pressure (unit: Pa), Q_m is the mass source (unit: kg/(m^3·s)).

(2) The modeled temperature field is controlled by the COMSOL's built-in "Heat Transfer in Porous Media" application modules, represented by following equations,

$$d_z(\rho C_p)_{eff}\frac{\partial T}{\partial t}+d_z\rho_f C_{p,f}u\cdot\nabla T+\nabla\cdot q=d_z Q+q_0 \quad (4)$$

$$q=-d_z k_{eff}\nabla T \quad (5)$$

$$k_{eff}=\varepsilon k_f+(1-\varepsilon)k_{pm} \quad (6)$$

$$□□□(\rho C_p)_{eff}=\varepsilon(\rho C_p)_f+(1-\varepsilon)(\rho C_p)_{pm} \quad (7)$$

where k_{eff} is the effective thermal conductivity (unit: W/(m·°C)), q_0 is the inward heat flux (unit: W/m^2), d_z is the rock thickness (unit: m), C_{peff} is the effective constant pressure heat capacity (unit: J/(kg·°C)), ε is the rock porosity (unit: 1), T is the temperature (unit: °C), Q is the heat source (unit: W/m^3), q is the thermal conductivity heat flow density (unit: W/m^2), u is the fluid velocity (unit: m/s), "f" and "pm" is fluid and porous matrix, respectively.

(3) The modeled mass conservation is controlled by the COMSOL's built-in "Dilute Matter Transfer" application modules, represented by following equations.

$$\frac{\partial（\varepsilon C_i）}{\partial t} + \frac{\partial（\rho C_i）}{\partial t} + \nabla \cdot J_i + u \cdot \nabla C_i = R_i \quad (8)$$

$$J_i = -D_i \nabla D_i \quad (9)$$

where c_i is the concentration (unit: mol/m^3), D_i is the diffusion coefficient (unit: m^2/s), R_i is the reaction rate of substance i (unit: mol/(m^3·s)), and J_i is the diffusion flux (unit: mol/(m^2·s))

(4) The chemical reaction proceeds as shown in equation (1), and the reaction rate is controlled by parameterizing the experimental data [26].

$$k=1.15\times10\text{-}5\times(70/a)^2 * pCO_2^{1/2} \times \exp[-0.000334*(T-185)^2] \quad (10)$$

Where k is the reaction rate (unit:1/s), a is the average effective grain size (unit: μm) , pCO_2 is the partial pressure of CO_2 (unit: 0.1 MPa) , and T is the temperature of the reaction region (unit: °C).

3. Results and analysis

Fig. 4 shows the simulation results on the peridotite carbonation at the typical case defined in the Table. 1, in which Fig. 4(a) shows the height-dependence of peridotite temperature distribution and (b) that of the annual average CO_2 sequestration per unit volume of peridotite (referring to the average CO_2 sequestration rate in kg/year·m³). It reveals the obvious drop in the temperature near the injection well, while gradual increase in other regions and similarly at the outer rocks near the peridotite region. The increase in the average peridotite temperature is found about 63°C from 185°C to 248°C after 730 days. Fig. 4 (b) regarding the average CO_2 sequestration rate was revealed to be less near the injection wells while that in the outer is zero because of its setting to be non-participation in the reaction. This is contrast to other areas with the almost homogeneous distribution of the average CO_2 sequestration rate, which gradually decreases because of its deviation from the optimal reaction temperature at 185°C. In this case, the average CO_2 sequestration rate can still achieve 123.71 kg/(year·m³) after 730 days. Results in Fig. 4 clearly represented the correlation between the peridotite temperature and the average CO_2 sequestration rate, as well as the reaction exothermic rate which affects back to the peridotite temperature and thus the reaction and heat. This study implies the crucial account of heat and mass transfer, also the initial peridotite temperature at 185°C seemly not achievable the fastest peridot carbonation rate. The CO_2 inflow temperature was found another factor critical to the CO_2 sequestration rate.

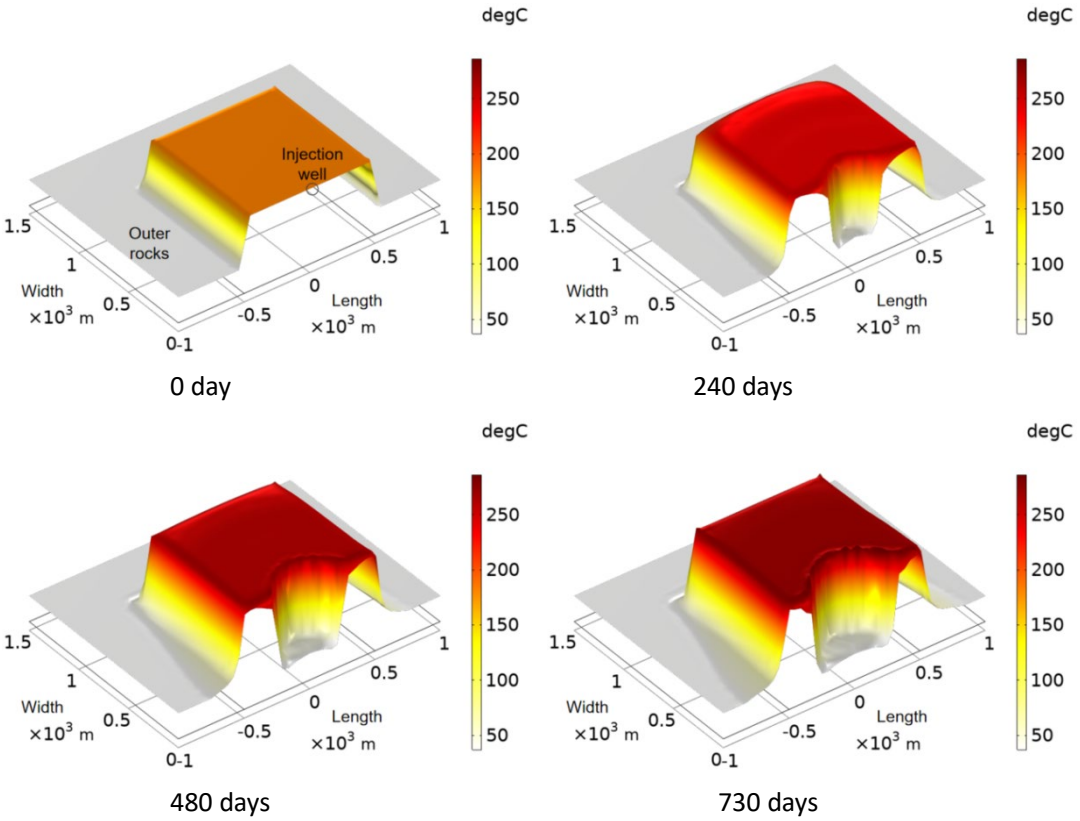

(a)

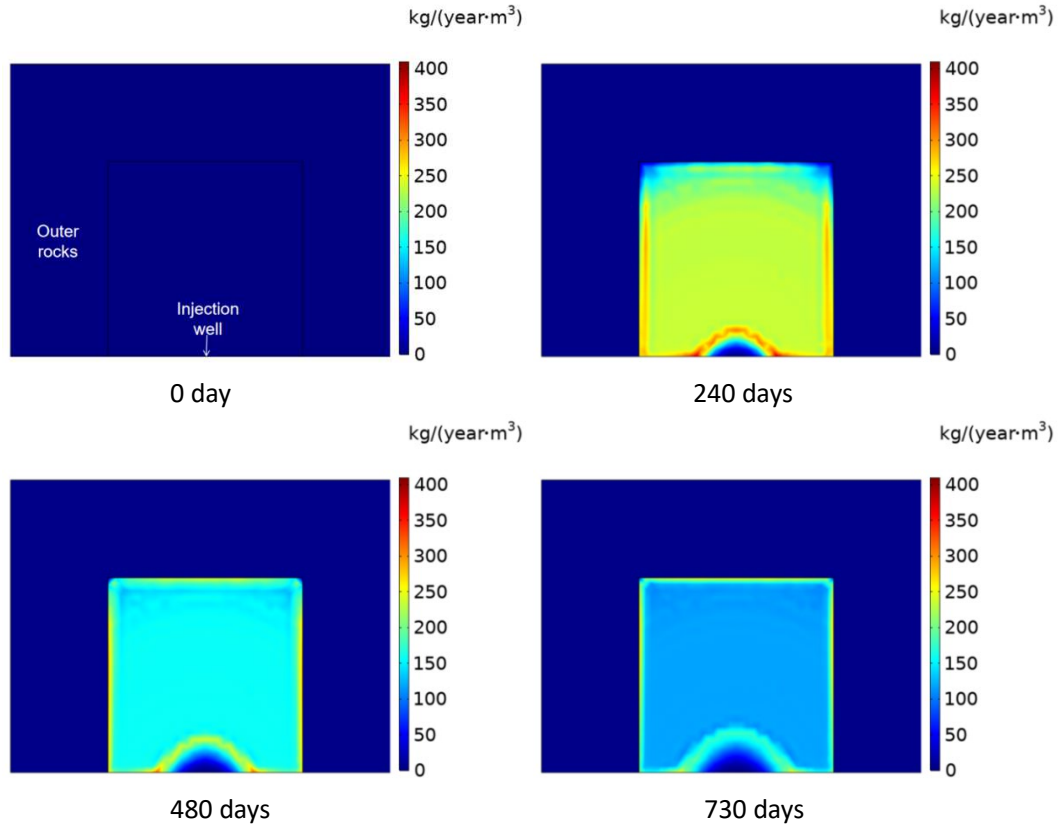

(b)

Fig. 4. Simulation results of peridotite carbonation process at the typical case as shown in the Table. 1 at different times, with (a) shows the height expression of peridotite temperature

distribution (°C), and (b) shows the distribution of annual average CO_2 sequestration per unit volume of peridotite (hereafter referred as average CO_2 sequestration rate, kg/year·m³).

Efforts have been made to improve the efficient use of exothermic heat, involving the investigation on effects of various temperature settings on the average CO_2 sequestration rate and the reaction exotherm rate. Fig. 5 shows the simulation results on the peridotite carbonation after 730 days when the CO_2 inflow temperature (Tin) and initial peridotite temperature (T0) were varied, respectively, which includes (a) regarding the average CO_2 sequestration rate (kg/year·m³) and (b) the average peridotite temperature (°C). Results in Fig. 5 (a) revealed the correlation of both too high or low T0 with to a decrease in the average CO_2 sequestration rate, and T0 seems even greater in affecting on the average CO_2 sequestration than Tin. The average CO_2 sequestration rate at a setting of Tin=T0=120°C achieves its maximum in 180.08 kg/year·m³, which is 43% higher than that of the typical case. Fig. 5 (b) reveals that the increase of Tin and T0 can gradually increase the average peridotite temperature and T0 has a greater effect on the average peridotite temperature than Tin. Upon a setting Tin=T0=120°C, the average peridotite temperature can achieve 245°C. It's interesting to see that the increased Tin and T0 does not imply a higher average CO_2 sequestration rate and exotherm heat rate. It's noticeable that temperature setting Tin=T0=90-150°C results in an optimal average CO_2 sequestration rate and the average peridotite temperature rise. This temperature setting coincides to that in the medium-temperature geothermal condition and the exhaust temperature of many carbon capture processes.

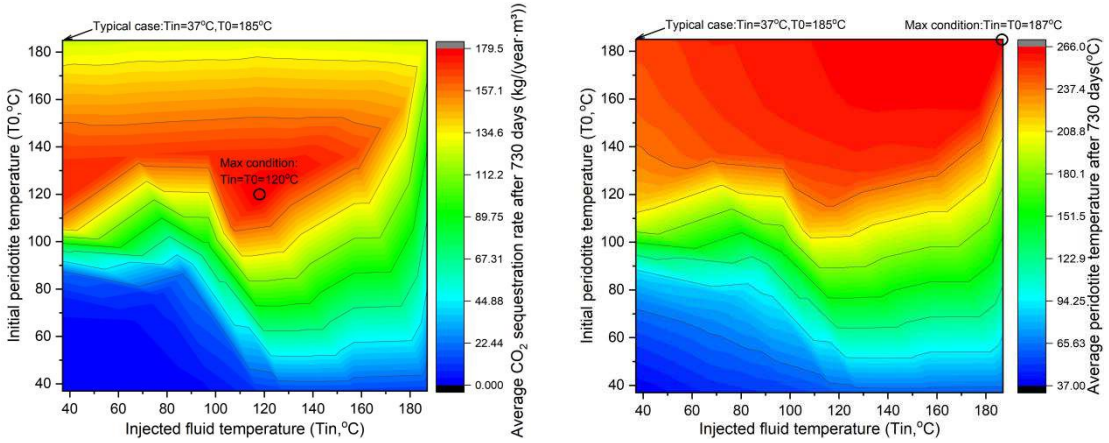

a b

Fig. 5. Simulation results after 730 days of peridotite carbonation when the fluid inflow temperature (Tin), initial peridotite temperature (T0) were varied, respectively, with (a) shows the average CO_2 sequestration rate (unit: kg/(year·m³)), and (b) shows the average peridotite temperature (temperature unit: °C).

Efforts have been done on the average CO_2 sequestration rate (kg/year·m³) and average peridotite temperature (°C) upon the varied Tin=T0 from 90 to 150°C compared to those at the typical case (Tin=37°C, T0=185°C). Results are shown in Fig. 6. The average CO_2 sequestration rate for both the typical case and the case of Tin=T0=90-150°C shows a peak shape over time, and the larger T0 the earlier the peak appears. The average peridotite temperature for both the typical case and Tin=T0=90-150°C are similarly increasing over time, but different in the extent of

temperature rise. Among of them, the average peridotite temperature for a setting at Tin=T0=120°C achieves by 125°C. Below this temperature, such as the setting at Tin=T0=90-100°C the peridotite temperature rise is very similar to that at the typical case. Alternatively, the setting at Tin=T0=110-150°C achieves the increase of the average CO_2 sequestration rate by 29~45% and the average peridotite temperature to be 229-259°C, respectively, which implies a temperature rise of 119~125°C over their respective initial peridotite temperature. Therefore, the setting at Tin=T0=110-150°C seems optimal in a higher average CO_2 sequestration rate and average peridotite temperature rise. This is equivalent to shift a medium-temperature geothermal (90-150°C) to a high-temperature geothermal (>150°C).

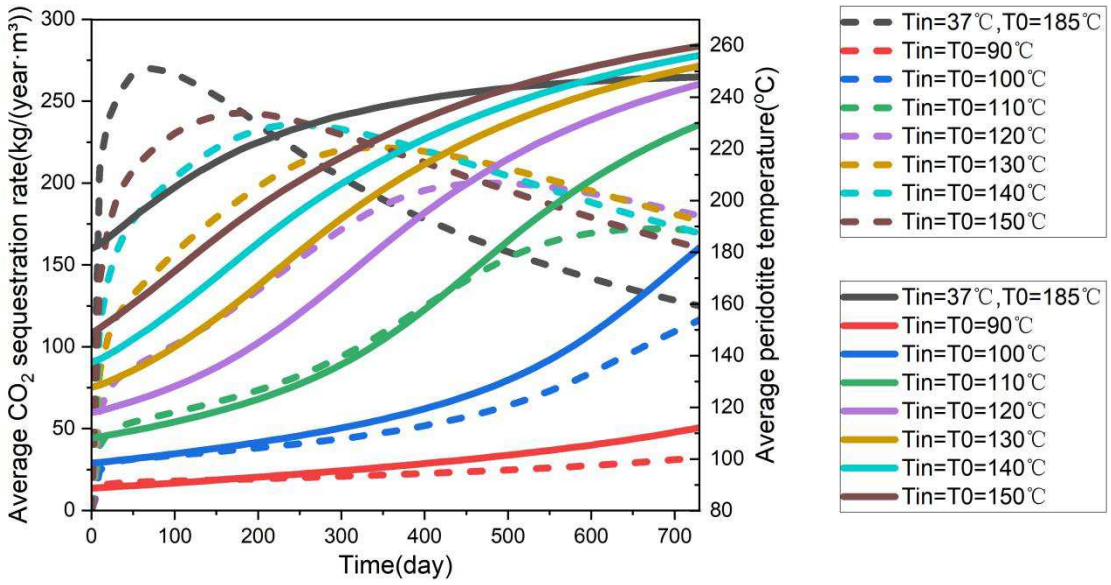

Fig. 6. The average CO_2 sequestration rate (unit: kg/(year·m³)) and average peridotite temperature (unit: °C) versus time for varying fluid inflow temperature (Tin) and initial peridotite temperature (T0) from 90 to 150°C versus the typical case (Tin=37°C, T0=185°C).

The previous investigation helps in estimating the CO_2 sequestration scale and its economics. It's reported that the annual CO_2 capture in 123,000 tons demands a forest in an area of 353 km² in the northwest China [27], contrasting to only demand for a peridotite volume in 1 km² when the geological peridotite formation at the aforementioned typical case is applied. Alternatively, the carbon emission intensity from a coal-fired power plant is 0.746 t CO_2/MW·h, and thus the total carbon emission in a 20-year period from a 600 MW coal-fired power plant demands for the geological peridotite formation of 160 m in thickness at its typical injection case. This only accounts for one 82nd of the geological peridotite formation which is found in Shaoguan City of Guangdong Province in China.

Since the CO_2 sequestration via the geological mineral CO_2 carbonation is similar to that via the deep saline formation (DSF), and thus the cost analysis of DSF can be a reference to estimate that in the the geological mineral CO_2 carbonation[28-30]. Assuming a 20-year injection term and negligible cost of waste heat and available nearby Supplementary facilities, the cost of the geological mineral CO_2 carbonation at its typical case can be calculated as \$4.492-8.838/t CO_2. In a case of setting at Tin=T0=110-150°C, the cost of the geological mineral CO_2 carbonation can be reduced to \$2.926-6.085/t CO_2 with the fluctuation depending on the injection conditions. As

shown in Fig. 7, the costs derived from the injection well construction and the injection activity jointly accounts for the greatest portion of the total cost, which is the similar to those in most geological projects.

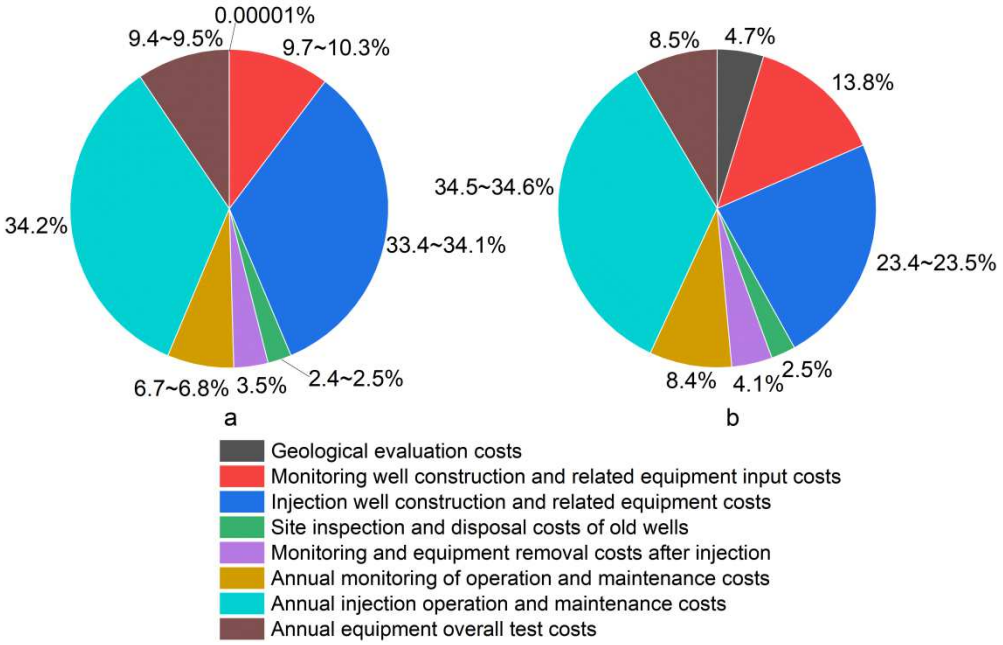

Fig. 7. Pie chart of the cost share of the sequestration process (unit: %), with (a) shows the case with no cost-sharing facilities, and (b) shows the case with surrounded by the cost-sharing facilities.

The carbon capture and storage (CCS) process consumes a lot of energy in the ground facilities maintenance and their operation, generating additional carbon emissions. It's fortunate that the current geological mineral CO_2 carbonation can generate heat to be used for the electricity generation, helping the CCS energy-saving and emission reduction. The expenses and benefits of CCS applying the geological mineral CO_2 carbonation technologies for current general case and future best case has been listed in the Supplementary Information Table. S2 (SI Table. 2)(calculated at 0.6 RMB/kWh electricity price, \$1 = 6.6RMB) [31-34]. Under current carbon price of its emission allowance in China (the current general case), If the efficiency of thermoelectricity from the geological mineral CO_2 carbonation process at its typical case is regularly 4%, the cost would be \$25.041/t CO_2 with no surrounding cost-sharing facilities, contrasting to an alternative profit of \$24.096/t CO_2 with available cost-sharing facilities and the thermoelectric efficiency at 10% at an optimally-applied temperature setting as well as the China's carbon price matching to that of international level (the future best case). The bright perspective oon the geological mineral CO_2 carbonation is revealed by wide distribution of rocks which are less deep than those of high-temperature geothermal (temperature>150°C). In the typical case of this study, the average temperature of "the artificial geothermal heat" can reach up to 248°C upon the CO_2 sequestration, equivalent to 40-56% reduction of the total geothermal mining cost compared to that in the regular geothermal [35,36].

Compared to other geological storage methods, the geological mineral CO_2 carbonation are very cost-competitive when operated under its favorable conditions. This is evidenced by a project in Iceland demonstrating profitable potentials of the mineral carbonation process to co-capture and

store other acid gases (e.g., H_2S and SO_2). Even more, another geological rock formation, basalt, shows more advantages in the mineral carbonation, which exists in both igneous reservoirs and geothermal fields [37,38]. Its economics and the implementation approach will be further discussed in details in our subsequent paper.

5. Conclusions

This study established a two-dimensional numerical simulation on the CO_2 mineral carbonation in peridotite, and evaluate its perspective economics, leading the following conclusion,

(1) The geological rock formations, such as alkali-silicates in peridotite, can be utilized for the permanent and stable CO_2 sequestration via the new "geological mineral CO_2 carbonation" into stable carbonates. This mineral carbonation reaction can be accelerated by means of the optimization of the CO_2 injections. Furthermore, the exothermic nature of the mineral carbonation reaction can release recoverable heat which can potentially compensate the energy consumption during the CO_2 sequestration.

(2) In a case of the initial temperature of the geological peridotite formation at 185^{o}C and that of the fluid inflow CO_2 at 37^{o}C, the average temperature elevation of peridotite by over 60 ^{o}C (reaching 248^{o}C) after 2 years. The average CO_2 sequestration rate in peridotite can achieve 123.71 kg/(year·m^3) in that case, meaning that the permanent sequestration of CO_2 generated from a 600 MW coal-fired power plant within its 20-year operation only demands a geological peridotite formation of 1 km^2 in its area and 160 m in its thickness.

(3) By changing both the fluid inflow temperature and the initial peridotite temperature to be 110~150^{o}C, the average CO_2 sequestration rate can be increased by 29~45% compared to that in the typical case, and leads to a temperature rise of 81~125^{o}C after 2 years, achieving a high-temperature geothermal condition which the temperature is greater than 150^{o}C.

(4) Heat production from the geological mineral CO_2 carbonation can profitably compensate the energy consumption in the carbon capture and storage (CCS) projects, and leading a shift of an expense in \$25.041/t CO_2 in China (the current general case) to an earning in \$24.096/t CO_2 in a best case at the price of the global carbon emission allowance converge.

ACKNOWLEDGMENT

The authors gratefully acknowledge the financial support of the NSFC (22178339), the Hundred Talents Program (A) of Chinese Academy of Sciences (2019).

References

1 Veal, A. J. Climate change 2021: the physical science basis, 6th report. *World Leisure Journal* **63**, 443-444, doi:10.1017/9781009157896 (2021).

2 Min, S. K., Zhang, X., Zwiers, F. W. & Hegerl, G. C. Human contribution to more-intense precipitation extremes. *Nature* **470**, 378-381, doi:10.1038/nature09763 (2011).

3 Stuart-Smith, R. F., Roe, G. H., Li, S. & Allen, M. R. Increased outburst flood hazard from Lake Palcacocha due to human-induced glacier retreat. *Nature Geoscience* **14**, 85-90, doi:10.1038/s41561-021-00686-4 (2021).

4 van Vuuren, D. P. *et al.* RCP2.6: exploring the possibility to keep global mean temperature increase below 2 degrees C. *Clim. Change* **109**, 95-116, doi:10.1007/s10584-011-0152-3

(2011).

5 Zhao, X., Ma, X., Chen, B., Shang, Y. & Song, M. Challenges toward carbon neutrality in China: Strategies and countermeasures. *Resources, Conservation and Recycling* **176**, doi:10.1016/j.resconrec.2021.105959 (2022).

6 Tang, X. *et al.* Carbon pools in China's terrestrial ecosystems: New estimates based on an intensive field survey. *Proc Natl Acad Sci U S A* **115**, 4021-4026, doi:10.1073/pnas.1700291115 (2018).

7 Davis, S. J. *et al.* Net-zero emissions energy systems. *Science* **360**, 1419-+, doi:10.1126/science.aas9793 (2018).

8 White, S. P. *et al.* Simulation of reactive transport of injected CO2 on the Colorado Plateau, Utah, USA. *Chem Geol* **217**, 387-405, doi:10.1016/j.chemgeo.2004.12.020 (2005).

9 Alcalde, J. *et al.* Estimating geological CO2 storage security to deliver on climate mitigation. *Nature Communications* **9**, doi:10.1038/s41467-018-04423-1 (2018).

10 Seifritz, W. CO_2 Disposal by Means of Silicates. *Nature* **345**, 486-486, doi:DOI 10.1038/345486b0 (1990).

11 Aradottir, E. S. P. & Hjalmarsson, E. in *International Carbon Conference (ICC).* 115-120 (2018).

12 Matter, J. M. *et al.* Rapid carbon mineralization for permanent disposal of anthropogenic carbon dioxide emissions. *Science* **352**, 1312-1314, doi:10.1126/science.aad8132 (2016).

13 Teir, S., Eloneva, S., Fogelhohn, C. J. & Zevenhoven, R. Stability of calcium carbonate and magnesium carbonate in rainwater and nitric acid solutions. *Energ Convers Manage* **47**, 3059-3068, doi:10.1016/j.enconman.2006.03.021 (2006).

14 Matter, J. M. & Kelemen, P. B. Permanent storage of carbon dioxide in geological reservoirs by mineral carbonation. *Nature Geoscience* **2**, 837-841, doi:10.1038/ngeo683 (2009).

15 Gislason, S. R. *et al.* Mineral sequestration of carbon dioxide in basalt: A pre-injection overview of the CarbFix project. *International Journal of Greenhouse Gas Control* **4**, 537-545, doi:10.1016/j.ijggc.2009.11.013 (2010).

16 Kelemen, P. B. *et al.* Rates and Mechanisms of Mineral Carbonation in Peridotite: Natural Processes and Recipes for Enhanced, in situ CO2 Capture and Storage. *Annual Review of Earth and Planetary Sciences* **39**, 545-576, doi:10.1146/annurev-earth-092010-152509 (2011).

17 Gadikota, G., Matter, J., Kelemen, P., Brady, P. V. & Park, A.-H. A. Elucidating the differences in the carbon mineralization behaviors of calcium and magnesium bearing alumino-silicates and magnesium silicates for CO2 storage. *Fuel* **277**, doi:10.1016/j.fuel.2020.117900 (2020).

18 Zhang, Q., Wang, Y., Zhou, G. Q., Qian, Q. & Robinson, P. T. in *Fall Meeting of the American-Geophysical-Union.* 541-566 (2003).

19 Kelemen, P. B. & Matter, J. In situ carbonation of peridotite for CO2 storage. *P Natl Acad Sci USA* **105**, 17295-17300, doi:10.1073/pnas.0805794105 (2008).

20 Rosa, D. R. N. & Rosa, R. N. Heat as a by-product or sub-product of CO2 storage in mafic and ultramafic rocks. *Int J Global Warm* **4**, 305-316, doi:Doi 10.1504/Ijgw.2012.049435 (2012).

21 Fang, H. H., Sang, S. X. & Liu, S. Q. Numerical simulation of enhancing coalbed methane recovery by injecting CO2 with heat injection. *Petroleum Science* **16**, 32-43, doi:10.1007/s12182-018-0291-5 (2019).

22 Rudge, J. F., Kelemen, P. B. & Spiegelman, M. A simple model of reaction-induced cracking applied to serpentinization and carbonation of peridotite. *Earth and Planetary Science Letters*

291, 215-227, doi:10.1016/j.epsl.2010.01.016 (2010).

23 Nasir, S. *et al.* Mineralogical and geochemical characterization of listwaenite from the Semail Ophiolite, Oman. *Chem Erde-Geochem* **67**, 213-228, doi:10.1016/j.chemer.2005.01.003 (2007).

24 Clark, D. E. *et al.* CarbFix2: CO2 and H2S mineralization during 3.5 years of continuous injection into basaltic rocks at more than 250 degrees C. *Geochim Cosmochim Ac* **279**, 45-66, doi:10.1016/j.gca.2020.03.039 (2020).

25 Zhang, C. *et al.* Radiogenic heat production variations in the Gonghe basin, northeastern Tibetan Plateau: Implications for the origin of high-temperature geothermal resources. *Renewable Energy* **148**, 284-297, doi:10.1016/j.renene.2019.11.156 (2020).

26 O'Connor W K, D. D. C., Rush G E, et al. Aqueous mineral carbonation. doi:10.13140/RG.2.2.23658.31684 (2005).

27 Qiu, Z., Feng, Z., Song, Y., Li, M. & Zhang, P. Carbon sequestration potential of forest vegetation in China from 2003 to 2050: Predicting forest vegetation growth based on climate and the environment. *Journal of Cleaner Production* **252**, doi:10.1016/j.jclepro.2019.119715 (2020).

28 Law, D. H. S. & Bachu, S. Hydrogeological and numerical analysis of CO2 disposal in deep aquifers in the Alberta sedimentary basin. *Energ Convers Manage* **37**, 1167-1174, doi:10.1016/0196-8904(95)00315-0 (1996).

29 Agency, U. S. E. P. United State Environment Protection Agency. Geologic CO2 sequestration technology and cost analysis. (United State Environment Protection Agency, Washington DC, 2008).

30 Heddle G, H. H., Klett M. The economics of CO2 storage. (Massachusetts Institute of Technology, Massachusetts, 2003).

31 Cai B F, L. Q., Zhang X, et al.,. China Carbon Dioxide Capture, Utilization and Storage (CCUS) Annual Report (2021) -- Study on the CCUS pathway in China (Institute of Environmental Planning, Chinese Ministry of Ecology and Environment, Institute of Rock and Soil Mechanics, Chinese Academy of Sciences, China Agenda 21 Management Center 2021).

32 Wang, X. *et al.* Cleaner coal and greener oil production: An integrated CCUS approach in Yanchang Petroleum Group. *International Journal of Greenhouse Gas Control* **62**, 13-22, doi:10.1016/j.ijggc.2017.04.001 (2017).

33 Alegria, P., Catalan, L., Araiz, M., Rodriguez, A. & Astrain, D. Experimental development of a novel thermoelectric generator without moving parts to harness shallow hot dry rock fields. *Applied Thermal Engineering* **200**, doi:10.1016/j.applthermaleng.2021.117619 (2022).

34 Kraemer, D. *et al.* High thermoelectric conversion efficiency of MgAgSb-based material with hot-pressed contacts. *Energy & Environmental Science* **8**, 1299-1308, doi:10.1039/c4ee02813a (2015).

35 FENG C G, L. S. W., WANG L S, et al. Present‐day geothermal regime in Tarim basin, northwest China. *Chinese Journal of Geophysics*, 2752-2762, doi:10.3969/j.issn.0001-5733.2009.11.010 (2009).

36 Bu, X., Ma, W. & Li, H. Geothermal energy production utilizing abandoned oil and gas wells. *Renewable Energy* **41**, 80-85, doi:10.1016/j.renene.2011.10.009 (2012).

37 Hu, T. *et al.* Oil origin, charging history and crucial controls in the carboniferous of western Junggar Basin, China: Formation mechanisms for igneous rock reservoirs. *Journal of Petroleum Science and Engineering* **203**, doi:10.1016/j.petrol.2021.108600 (2021).

38 Erol, S., Akın, T., Başer, A., Saraçoğlu, Ö. & Akın, S. Fluid-CO2 injection impact in a geothermal reservoir: Evaluation with 3-D reactive transport modeling. *Geothermics* **98**, doi:10.1016/j.geothermics.2021.102271 (2022).

Supplementary Files

This is a list of supplementary files associated with this preprint. Click to download.

- SupplementaryInformationtheGeologicalMineralCO2CarbonationCY06142022.docx